Statetostate rate constants for quenching of xenon 6p levels by rare gases

W. J. Alford

Citation: The Journal of Chemical Physics **96**, 4330 (1992); doi: 10.1063/1.462862
View online: http://dx.doi.org/10.1063/1.462862
View Table of Contents: http://scitation.aip.org/content/aip/journal/jcp/96/6?ver=pdfcov
Published by the AIP Publishing

State-to-state rate constants for quenching of xenon 6*p* levels by rare gases

W. J. Alford
Sandia National Laboratories, Albuquerque, New Mexico 87185

(Received 29 July 1991; accepted 20 November 1991)

State-to-state rate constants have been measured for xenon $6p[3/2]_{1,2}$, $6p[5/2]_{2,3}$, $6p[1/2]_1$, and $6s'[1/2]_1$ levels quenched by helium, neon, argon, and xenon. Some total rate constants and 6*p* radiative transition probabilities have also been measured. The time-dependent fluorescence from pumped and collisionally populated levels following pulsed excitation of a single level is observed. Data for different gas pressures are fit using a rate equation model that includes all relevant levels. Neon is found to have small total rate constants, while xenon has large total rate constants. Both neon and xenon quench to a number of nearby levels. Helium and argon have total rate constants varying greatly with 6*p* level. Helium tends to quench to the next lower level while argon usually quenches to many levels.

I. INTRODUCTION

Collisional relaxation of excited states of rare gases has been studied recently by a number of groups.[1-13] The interest is due to the importance of rare gas excited states in high pressure (>0.5 atm) discharges involving rare gases. Excimer and xenon lasers are two important systems where an understanding of the laser gas kinetics requires an understanding of rare gas excited-state collisions. Recent measurements[11] and modeling[14,15] have shown that the lasing spectrum of high pressure atomic xenon lasers is determined largely by quenching of the lower laser levels.

In addition to being of practical interest in discharges, collisions of excited states in general have been a topic of much work.[16] Studies of fine-structure changing collisions in alkali-rare gas systems[17] and group II-rare gas systems[18] are common. Xenon is of interest because the *jK* coupling scheme applicable to xenon is different from the LS coupling applicable to the group I and II elements. The large number of electrons poses a real challenge in calculating interatomic potentials. Additionally, the fine structure splitting is rather large (see Fig. 1) and must be calculated accurately in the separated-atoms limit of the potentials.

The first studies of quenching of xenon 6*p* levels were conducted by Horiguchi *et al.*[1] Initially, total rate constants were emphasized. Later studies measured more total and some state-to-state rate constants.[2-12] The room-temperature rate constants for quenching the 6*p* levels can be rather large ($\sim 10^{-10}$ cm^3 s^{-1}) since nearby levels are within a few hundred wave numbers or less. Quenching by xenon is the most studied system, but there remain gaps in the understanding of this system. Total quenching rates for argon and krypton have been obtained recently[6,9-11] and state-to-state rate constants have been obtained very recently for some 6*p* levels.[10] For helium and neon, some total rate constants[11,12] and a few state-to-state rate constants[12] have been measured.

This paper presents studies of the lower five 6*p* levels and the $6s'[1/2]_1$ level which is just 84 cm^{-1} below the $6p[1/2]_1$ level. [The prime designates a $5p^5(^2P_{1/2})$ core, while the other states have a $5p^5(^2P_{3/2})$ core.] The highest 6*p* level $6p[1/2]_0$ is not studied because of the difficulty of detecting 5*d* levels which can be strongly coupled to it by collisions. Helium, neon, argon, and xenon gases are studied as quenchers. Short pulse excitation of individual 6*p* levels is provided by two-photon excitation and fluorescence from the pumped level as well as the collisionally populated levels is observed. We have measured total and state-to-state rate constants by fitting the time dependence and relative amplitudes of the observed fluorescence. A discussion of the experiment is given in Sec. II. The results are presented in Sec. III and discussed in Sec. IV.

II. EXPERIMENT

The experimental setup is shown in Fig. 2 and is similar to that used in our earlier measurements.[11] Light from a

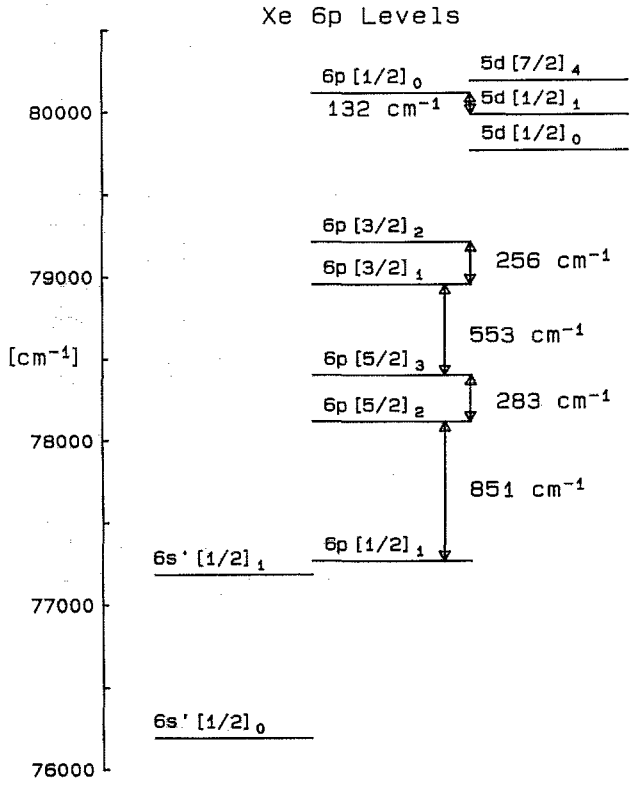

FIG. 1. A partial energy level diagram of atomic xenon showing the 6*p* manifold and nearby levels.

 0021-9606/92/064330-11$06.00

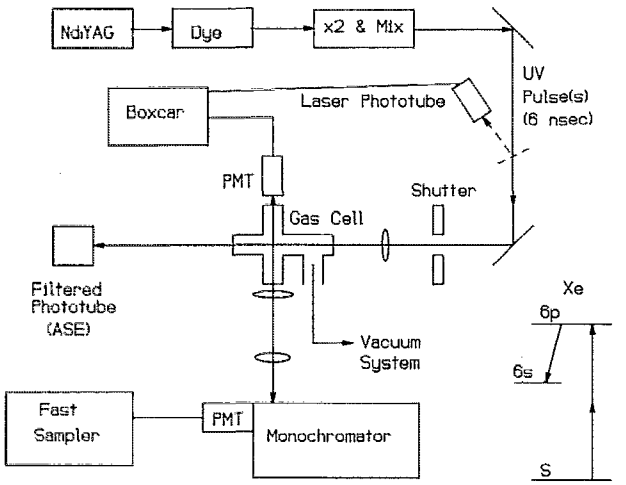

FIG. 2. Experimental setup.

Nd:YAG pumped dye laser is frequency doubled and mixed with 1.06 μ light in a KDP crystal to produce the UV wavelengths required for two-photon pumping the 6p levels. We individually pump the 6p[3/2]$_{1,2}$, 6p[5/2]$_2$, and 6p[1/2]$_1$ levels. The 6p[5/2]$_3$ level is not readily pumped by two photons from the ground state because the transition is dipole forbidden ($\Delta J = 3$). Due to selection rules, the $J = 1$ 6p levels (6p[3/2]$_1$ and 6p[1/2]$_1$) require pumping with two different wavelength photons having orthogonal polarizations. For these levels, the doubled-dye and doubled-dye plus 1.06 μ wavelengths are both used. The ~6 ns wide UV pulses are gently focused into a stainless-steel, room-temperature (295 K) gas cell containing the gases of interest. A long focal length (50–100 cm) spherical lens or a cylindrical lens (focal length of 20–50 cm) was used to focus the laser pulses. Often the observation region was near, but not exactly at the beam focus in order to reduce the laser intensity. The gas cell

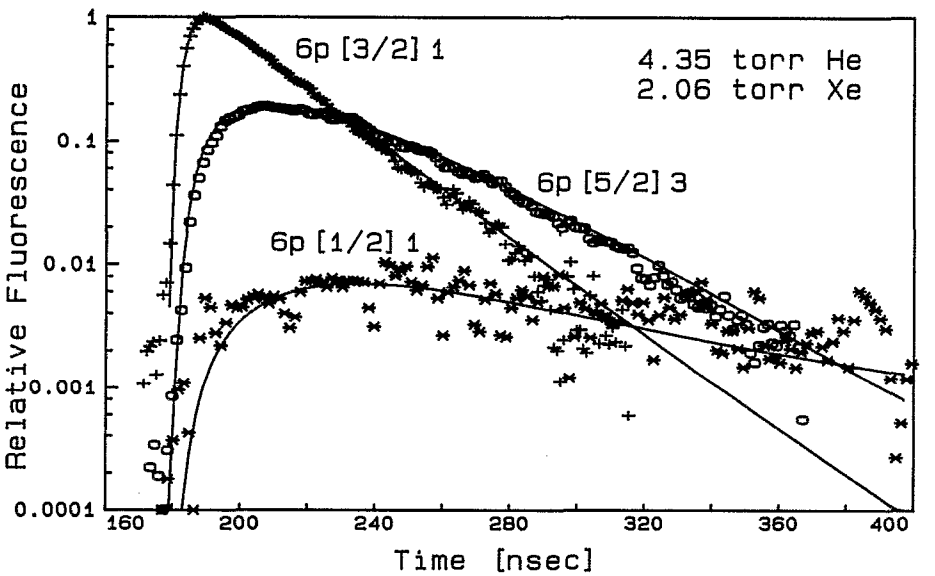

FIG. 3. Fluorescence following 6p[3/2]$_1$ excitation. The symbols are experimental data. The curves are obtained by modeling the fluorescence with state-to-state rate constants determined in this work.

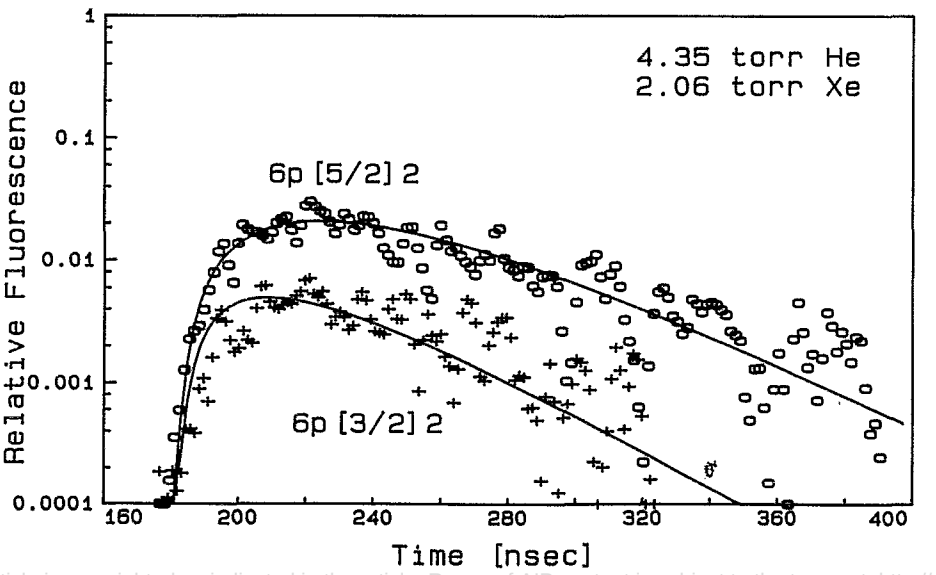

was routinely pumped down to $\sim 10^{-7}$ Torr before being filled with high purity rare gas. Stated purities were helium—99.999%, neon—99.996%, argon—99.999%, and xenon—99.999%. Pressures in the cell are measured within 1% with MKS 122*A* Baratron pressure transducers.

Fluorescence from the pumped and the collisionally populated $6p$ levels to the $6s[3/2]_{1,2}$ levels was monitored by two photomultipliers (PMTs). Both PMTs (Hamamatsu R632-01) have *S*-1 photocathodes for reasonable red response. The first PMT used filters to isolate fluorescence from the $6p$ manifold and its output was recorded by a gated integrator. The second PMT was connected to a 0.33 m monochromator and detected the spectrally resolved $6p$ fluorescence. The output of the second PMT is recorded using a fast sampler (SRS model 255) whose 1 ns gate is scanned in time so that over many laser pulses, a fluorescence decay was obtained. To remove pulse-to-pulse amplitude variations, the signal of the time-scanned PMT is normalized by the first PMT. A shutter is closed to obtain baseline signals. Care must be taken to not pump the $6p$ levels too hard or the xenon can be ionized by a third photon and the subsequent ion–electron recombination would give spurious $6p$ fluorescence signals.[19] In addition, amplified spontaneous emission (ASE) from the pumped level can redistribute populations. A filtered phototube was used to monitor $6p$ ASE to the $6s$ levels in the forward direction. Data is obtained under conditions where $6p[1/2]_0$ fluorescence (pumped by ion–electron recombination if laser intensities are too large) is negligible and where ASE signals are very small or unobservable.

A relative calibration of the monochromator/PMT system sensitivity as a function of wavelength was obtained using a calibrated quartz–iodine lamp. The $6p$–$6s$ fluorescence lies between 8200 Å and 1.084 μ. Over this range, the monochromater/PMT sensitivity varied by a factor of 3. The lamp output is rather flat in this region and the relative calibration is accurate to 10%.

An example of data obtained when pumping the $6p[3/2]_1$ level is given in Fig. 3. The data have been corrected for monochromator/PMT sensitivy. The curves shown are obtained using a rate equation model of the laser pumping and collisional and radiative decay of the $6p$ and $6s'$ levels. The model includes the $6p[3/2]_{1,2}$, $6p[5/2]_{2,3}$, $6p[1/2]_1$, $6s'[1/2]_{1,2}$, and $6s[3/2]_1$ levels. The model allows radiative relaxation of each $6p$ level to the $6s[3/2]_1$ level at a rate equal to the radiative rate of the $6p$ level. (In the model, emission to $6s[3/2]_2$ is treated as if it were emission to $6s[3/2]_1$.) Each level in the model is collisionally coupled to all other levels in the model by all gases present. The rate equations are integrated using the fourth-order Runge–Kutta method. The $6s[3/2]_1$ level is included to close the system, i.e., no population is transferred to levels not in the model. Experimentally, we do not distinguish between the $6s[3/2]_{1,2}$ levels. Thus in the model, $6s[3/2]_1$ represents all levels below the $6s'$ levels. Due to the large energy gap ($> 8000\,\mathrm{cm}^{-1}$) between the levels of interest and the $6s$ levels, this is a reasonable approximation since virtually no population goes back to the $6p$ or $6s'$ levels once it reaches the $6s$ levels. Total radiative rates are obtained from known lifetimes. To convert the populations given by the rate equations to relative fluorescence intensities, the radia-

TABLE I. Transition probabilities for xenon ($10^6\,\mathrm{s}^{-1}$).[a]

Transition	Wavelength (Å)	Transition probabilities ($10^6\,\mathrm{s}^{-1}$)	
		This work	Others
$6p[3/2]_2$–$6s[3/2]_2$	8 234	25.1 ± 0.8	18.6,[b] 28.6 ± 1.3[c] 3.8,[d] 13,[f] 29[f] 23,[g] 22.4[h]
$6p[3/2]_2$–$6s[3/2]_1$	8 955	8.21 ± 0.8	7.9,[b] 7.50 ± 0.71[c] 8,[e] 11,[g] 9.42[h]
$6p[3/2]_1$–$6s[3/2]_1$	9 165	27.0 ± 0.6	27.7,[b] 21.7 ± 2.4[c] 25,[g] 26.3[h]
$6p[3/2]_1$–$6s[3/2]_2$	8 412	1.45 ± 0.4	2.5,[b] 3.06 ± 0.13[c] 0.83,[d] 2.1,[g] 2.31[h]
$6p[5/2]_2$–$6s[3/2]_1$	9 926	18.0 ± 0.8	15.9,[b] 12.0 ± 1.2[c] 10,[g] 17.4[h]
$6p[5/2]_2$–$6s[3/2]_2$	9 048	9.47 ± 0.8	9.1,[b] 12.4 ± 0.6[c] 13.8,[f] 13,[g] 9.72[h]
$6p[1/2]_1$–$6s[3/2]_2$	9 802	25.3 ± 1.0	24.8,[b] 31.1 ± 1.4[c] 26.6,[f] 21,[g] 23.9[h]
$6p[1/2]_1$–$6s[3/2]_1$	10 841	0.99 ± 0.4	2.5,[b] 1.70 ± 0.25[c] 0.97,[g] 1.37[h]

[a] Radiative lifetimes used to obain these results are given in the text.
[b] Horiguchi *et al.* (1981) (Ref. 1).
[c] Sabbagh and Sadeghi (1977) (Ref. 22).
[d] Miller and Roig (1973) (Ref. 23).
[e] Karimov and Klimkin (1971) (Ref. 24).
[f] Malakhov (1965) (Ref. 25).
[g] Chen and Garstang (1970) (Ref. 26).
[h] Aymar and Coulomb (1978) (Ref. 20) (velocity).

tive transition probabilities are needed. We have measured the required transition probabilities by measuring the branching ratios of emission from the $6p$ to $6s$ levels. The results will be discussed in the next section. The state-to-state quenching rate constants are determined by fitting the fluorescence data, as discussed below. Thus all radiative and collisional processes important for describing the observed fluorescence decays are included in the model except for coupling to higher energy states which should be small at room temperature.

Observation of the fluorescence transitions observed in Fig. 3 requires a dynamic range in fluorescence detection of greater than three orders of magnitude. We obtained this by varying the voltage applied to the PMT on the monochromator. We use the measured voltage-dependent gain to scale data obtained at different voltages. This has the advantage of being convenient, but has the disadvantage of distorting the late-time decays of large signals recorded with low PMT voltages, i.e., fluorescence decays of some pumped levels. This is noticeable in Fig. 3(a), where the $6p[3/2]_1$ data is systematically below the calculated curve at late times. When the signal is attenuated and a higher PMT voltage is used, the data and calculation agree very well. We were careful to take this into account when analyzing the data. A second effect arising from changing the PMT voltage is a slight change in the transit time of photoelectron pulses through the dynode structure of the PMT. Thus signals obtained at low voltage are delayed slightly in time relative to those obtained at high voltage. This effect was measured and corrections to the data have been made.

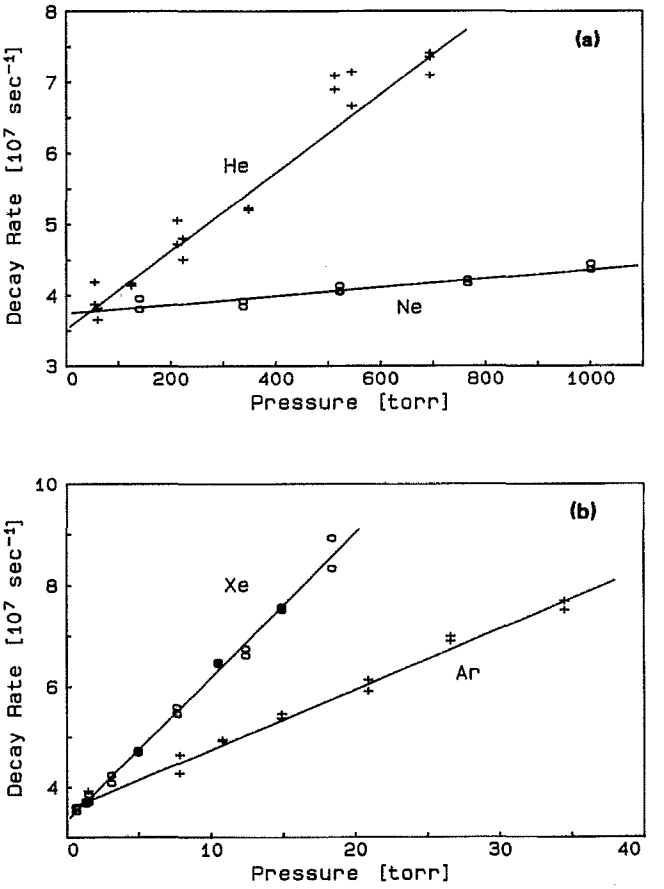

FIG. 4. Stern–Volmer plots for quenching the $6p[3/2]_2$ level by (a) helium and neon and (b) argon and xenon.

III. RESULTS

We first present the results for the radiative transition probabilities. The $6p$ levels can only fluoresce in the near IR to the $6s$ levels and in the IR to the $6s'$ levels. The transitions to the $6s$ levels are expected to have much higher transition probabilities than transitions to $6s'$ levels because the wavelengths are shorter and the core is the same as the $6p$ levels. Calculations support this expectation.[20] Thus to a good approximation, the lifetimes of the $6p$ levels are determined by $6p$ to $6s$ transitions. We have determined the transition probabilities of the $6p$ $J = 1,2$ levels by observing the relative fluorescence intensities to the $6s[3/2]_{1,2}$ levels while pumping the level of interest. This allows a determination of the radiative branching ratios to the $6s$ levels. From known radiative lifetimes, one can then obtain the individual $6p$ to $6s$ radiative transition probabilities. Our results are shown in Table I along with the results of other work. The radiative lifetimes of the $6p[3/2]_1$ and $6p[5/2]_2$ levels (35.1 and 36.4 ns, respectively) are taken from our previous work.[11] A lifetime of 38 ns is used for the $6p[1/2]_1$ level.[3,6] A lifetime of 30 ns has been measured in this work for the $6p[3/2]_2$ level and will be discussed shortly. The transition probabilities measured in this work qualitatively agree with previous values. That is, the stronger transition out of each $6p$ level is in general agreement. The actual transition probabilities, however, vary due to the use of different lifetimes and branching ratios. Most of the data used in determining the state-to-state rate constants reported in this work are based on the 8234, 9165, 9048, and 9802 Å transitions (see Table I for the transition designations). Some data used the 9926 Å $6p[5/2]_2$ emission and it is consistent with the 9048 Å emission data.

Total quenching rate constants for $6p[3/2]_2$ have been determined by measuring the fluorescence decay rate as a function of quenching-gas pressure. The resulting Stern–Volmer plots of the decay rate vs pressure are shown in Fig. 4. The slope of each curve gives the total quenching rate constant for that gas. These total rates are listed in Table II. The intercept for the Xe quenching data in Fig. 4(b) yields the radiative lifetime of the $6p[3/2]_2$ level—30.0 ± 1.5 ns. Our other total quenching rate constants in Table II were obtained from state-to-state data such as that shown in Fig. 3; no Stern–Volmer plots were made of this data. Instead, the state-to-state rate constants out of a given level, obtained by fitting all the fluorescence data with the rate equation model, are summed to yield a total rate constant. Total rate constants out of $6p[3/2]_1$ and $6p[5/2]_2$ determined previously by Stern–Volmer plots[11] were used as starting points in our fitting and generally agreed with the current results. The only exception is helium quenching of $6p[5/2]_2$ which displays a double-exponential decay when pumping $6p[5/2]_2$. The previous result[11] used only low pressure data where a single-exponential decay was thought to dominate. The current decay rate should be better since a single exponential is

TABLE II. Rate constants for quenching of some xenon levels (10^{-11} cm^3 s^{-1}) at 295 K.

Level	He	Ne	Ar	Xe
$6p$	2.0 ± 0.2[j]	0.2 ± 0.2[c]	20.0 ± 0.4[a]	0.59 ± 0.05[a]
$[1/2]_0$		3.4 ± 0.2[j]	14.0 ± 1.0[e]	0.42 ± 0.05[b]
				0.58 ± 0.05[c,e]
				0.59 ± 0.33[d]
				1.6 ± 0.4[h]
				40 ± 10[f]
$6p$	0.17 ± 0.08[j]	0.4 ± 0.2[c]	4.0 ± 0.1[a]	10.1 ± 0.3[a]
$[3/2]_2$	0.17 ± 0.03[m]	0.05 ± 0.03[j]	2.2 ± 0.2[c]	8.5 ± 0.5[b]
		0.019 ± 0.010[m]	4.7 ± 0.5[e]	8.2 ± 0.5[c,e]
			4.7 ± 0.5[g]	9.22 ± 0.47[d]
			3.7 ± 0.4[m]	8.7 ± 0.8[m]
$6p$	7.49 ± 0.32[k]	0.5 ± 0.2[c]	<0.5[g]	8.9 ± 2.6[d]
$[3/2]_1$	7.45 ± 0.40[m]	0.0386 ± 0.0066[k]	1.0 ± 0.3[i]	12.8 ± 0.4[e]
		0.033 ± 0.008[m]	0.176 ± 0.063[k]	11.3 ± 0.3[k]
			0.20 ± 0.03[m]	11.5 ± 0.6[m]
$6p$	~ 0.7[j]	0.5 ± 0.2[c]	1.3 ± 0.3[c]	3.92 ± 0.44[d]
$[5/2]_3$	1.0 ± 0.3[m]	~ 0.3[j]	3.0 ± 0.6[g]	5.3 ± 0.3[e]
		0.22 ± 0.10[m]	2.5 ± 0.6[i]	7.6 ± 1.5[m]
			5.1 ± 1.2[m]	
$6p$	0.9 ± 0.2[j]	0.3 ± 0.3[c]	8.2 ± 0.4[a]	11.6 ± 0.3[a]
$[5/2]_2$	0.65 ± 0.12[k]	0.8 ± 0.2[j]	8.2 ± 0.5[c]	8.68 ± 0.59[d]
	0.95 ± 0.2[m]	0.560 ± 0.020[k]	8.6 ± 0.5[i]	9.6 ± 0.3[e]
		0.57 ± 0.10[m]	7.87 ± 0.40[k]	10.1 ± 0.3[k]
			8.0 ± 0.4[m]	10.1 ± 0.5[m]
$6p$	$\leqslant 0.2$[j]	0.3 ± 0.3[c]	0.3 ± 0.3[c]	13 ± 2[c]
$[1/2]_1$	4.0 ± 2.0[m]	~ 0.3[j]	0.6 ± 0.3[i]	29.5 ± 4.8[d]
		0.035 ± 0.020[m]	0.74 ± 0.4[m]	13.3 ± 0.5[e]
				18.1 ± 5.0[m]
$6s'$	2.7 ± 1.3[m]	0.0135 ± 0.010[m]	0.85 ± 0.50[m]	6.65 ± 1.00[j]
$[1/2]_1$				10.1 ± 4.5[m]

[a] Bruce *et al.* (1990) (Ref. 9).
[b] Moutard *et al.* (1986) (Ref. 7).
[c] Inoue *et al.* (1984) (Ref. 3).
[d] Bowering *et al.* (1986) (Ref. 5)..
[e] Ku and Setser (1986) (Ref. 6).
[f] McCowan *et al.* (1982) (Ref. 2).
[g] Horiguchi *et al.* (1981) (Ref. 1).
[h] Karatazaev (1987) (Ref. 8).
[i] Xu and Setser (1990) (Ref. 10).
[j] Xu and Setser (1991) (Ref. 12).
[k] Alford (1990) (Ref. 11).
[l] Sadeghi and Sabbagh (1977) (Ref. 13).
[m] Present work.

not assumed. Indeed, our current value for quenching of $6p[5/2]_2$ is in better agreement with the value of Xu and Setser.[12] Our total rate constants usually agree with previous results within the combined uncertainties. However, there are some notable exceptions which will be discussed in the next section.

Our measured total quenching rate constants are summarized graphically in Fig. 5. Xe is seen to have rate constants of $\sim 10^{-10}$ cm^3 s^{-1} for all $6p$ levels studied. Neon, on the other hand, has rates about two orders of magnitude smaller ($< 6 \times 10^{-12}$ cm^3 s^{-1}). Helium and argon show an interesting anticorrelation—argon has large rate constants for $6p[3/2]_2$ and $6p[5/2]_{2,3}$, while helium has small rate constants. Argon has small rate constants for $6p[3/2]_1$ and $6p[1/2]_1$ and helium has large rate constants for those levels. This behavior helps explain the lasing spectrum of high pressure xenon lasers that use helium, neon, and argon as buffer gases.[11] These lasers operate on various $5d$–$6p$ transitions. Rapid quenching of a particular $6p$ level favors lasing that terminates on that level, since a high quenching rate is able to maintain the population inversion required for lasing.

The state-to-state quenching rate constants are obtained using the rate equation model described above. The rate constants are varied to obtain a best fit to the fluorescence data. Specifically, the state-to-state downward rate constants are adjusted to best fit data for several different pressures and for

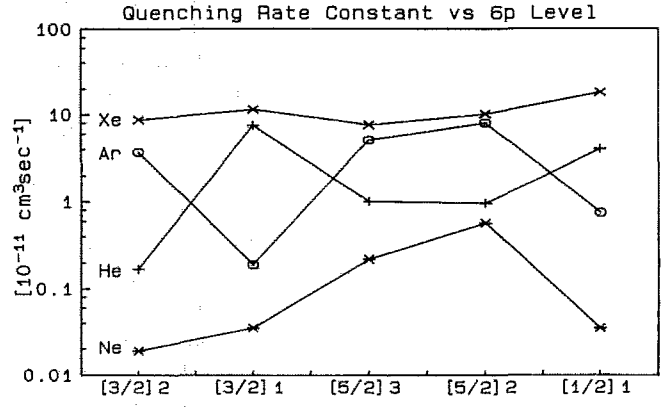

FIG. 5. Quenching rate constants vs the $6p$ level for helium, neon, argon, and xenon.

TABLE III. Gas mixes studied for state-to-state analysis. Partial pressures in Torr.

Pumped level	Xe	He	Ne	Ar
$6p[3/2]_2$	7.3, 14, 22			
	1.5	50, 100, 320		
	1.5			12, 21
	0.5			7.3
	1.1		554	
	1.5	15		11
$6p[3/2]_1$	6.8, 7.6, 8.3, 14, 22			
	2.0	18, 75		
	6.8	22		
	4.2	14		
	0.52	9.8		
	1.0		300, 540	
	2.0			100
	2.1	18		9.7
	0.54	8.4		12
	1.0	12	120	
	1.0	5.6	53	
$6p[5/2]_2$	5.1, 7.0, 7.9, 14, 22			
	2.0	67, 129		
	0.5	33, 87		
	1.1		46, 72, 21,	
	0.5		31, 49, 64	
	2.0			5.1, 10
	1.5			21
	0.5			9.2, 14
$6p[1/2]_1$	0.7, 1.5, 2.0, 3.2, 4.2, 8.5, 14, 26, 45, 76			
	1.5	9.7, 23, 41, 130, 160, 320		
	7.2	33		
	21	68		
	1.0		77, 61, 130	
	0.5		34, 140, 170, 220, 310, 420, 570	
	1.5			14, 33, 54, 99, 230, 420
	7.5			63
	2.0	26		48

various pumped levels. A total of 85 gas mixes/pumped level combinations were used and are shown in Table III. The upward rate constants are determined by detailed balance

$$k_{21} = k_{12}\,(g_1/g_2)\,\exp[-(E_1 - E_2)/kT],$$

where k_{ij} is the state-to-state rate constant for going from state i to state j, g_i is the degeneracy of state i, E_i is the energy of state i, and k is Boltzmann's constant. In principle, only a few fluorescence decays are required to determine all the state-to-state rate constants. In practice, however, a particular set of conditions is sensitive to a few rate constants and insensitive to most. Therefore, the pressures and mixtures as well as the pumped level are varied in an effort to cover conditions sensitive to each rate constant. The overall goodness of a fit is determined subjectively since data from many conditions are analyzed. Our set of state-to-state rate constants are shown in Tables IV and V along with previous measurements. The uncertainty of a particular rate constant is obtained by varying it until the fit obviously disagrees with the data, i.e., misses most of the data in a systematic way. The state-to-state rate constants with no stated uncertainty are very approximate and good to a factor of 3–10.

Data involving quenching of $6p[3/2]_2$ by helium suggests a small rate for quenching this level and/or $6p[3/2]_1$ to a higher, unidentified level not included in the model, probably a $5d$ level. This shows up as a poor fit to the late-time fluorescence decay of $6p[3/2]_2$ when pumping $6p[3/2]_1$, the fit being systematically below the data at late time. Since the higher level was not identified, a definite rate was not assigned to this process. However, the rate constant must be small compared to the total quenching rate constant of $6p[3/2]_2$.

The rate constants for $6p[1/2]_1$ require some explanation. Because the $6p[1/2]_1$ level is only 84 cm^{-1} above the

TABLE IV. State-to-state rate constants for quenching of xenon (10^{-11} cm^3 s^{-1}) at 295 K.

Initial level	Final level	Ar		Xe		
		a	*b*	*a*	*c*	*d*
$6p[3/2]_2$	$6p[3/2]_1$	0.11 ± 0.05	1.4 ± 0.2	1.1 ± 0.3	1.3 ± 0.2	0.64 ± 0.15
	$6p[5/2]_3$	~ 0.03	1.4 ± 0.2	2.9 ± 0.5	2.1 ± 0.2	2.24 ± 0.31
	$6p[5/2]_2$	0.5 ± 0.03	1.9 ± 0.2	2.8 ± 0.6	2.8 ± 0.2	2.65 ± 0.69
	$6p[1/2]_1$	0.10 ± 0.04		~ 0.01	< 0.2	
	$6s'[1/2]_1$	2.4 ± 0.5		~ 0.01		3.2 ± 1.4
	$6s'[1/2]_0$	~ 0.6		1.9 ± 0.6	1.9 ± 0.2	
$6p[3/2]_1$	$6p[5/2]_3$	0.03 ± 0.015	1.0 ± 0.2	9.6 ± 1.0	6.0 ± 2.0	
	$6p[5/2]_2$	~ 0.01		1.2 ± 0.5		
	$6p[1/2]_1$	0.065 ± 0.030		0.2 ± 0.2		
	$6s'[1/2]_1$	~ 0.04				
	$6s'[1/2]_0$				6.2 ± 2.0	
$6p[5/2]_3$	$6p[5/2]_2$	2.0 ± 0.9	2.6 ± 0.6	3.4 ± 0.4	3.1 ± 0.2	
	$6p[1/2]_1$	3.0 ± 1.0		1.8 ± 0.6	0.4 ± 0.2	
	$6s'[1/2]_1$	~ 0.1		~ 0.8	0.4 ± 0.2	
	$6s'[1/2]_0$			1.3 ± 0.7	1.4 ± 0.2	
$6p[5/2]_2$	$6p[1/2]_1$	5.8 ± 0.7	5.4 ± 1.0	3.7 ± 0.5	4.5 ± 0.2	4.6 ± 1.8
	$6s'[1/2]_1$	1.5 ± 0.7	2.3 ± 0.4[e]	1.5 ± 0.4	< 0.2	2.2 ± 0.8
	$6s'[1/2]_0$			3.7 ± 0.5	4.0 ± 0.2	
$6p[1/2]_1$	$6s'[1/2]_1$	0.4 ± 0.3	0.6 ± 0.3	10.0 ± 4.0	10.0 ± 2.0	
	$6s'[1/2]_0$	0.15 ± 0.10		6.0 ± 2.5	3.3 ± 2.0	
	$6s$	~ 0.005		2.0 ± 1.0		
$6s'[1/2]_1$	$6s'[1/2]_0$	0.55 ± 0.3		2.5 ± 1.5	0.7 ± 0.3	
	$6s$	~ 0.005		0.9 ± 0.5		
$6s'[1/2]_0$	$6s$	~ 0.005		0.9 ± 0.5		

[a] This work.
[b] Xu and Setser (1990) (Ref. 1).
[c] Ku and Setser (1986) (Ref. 6).
[d] Bowering *et al.* (1986) (Ref. 4).
[e] Combined $6s'[1/2]_1$ and $6s'[1/2]_0$.

TABLE V. State-to-state rate constants for quenching of xenon (10^{-11} cm^3 s^{-1}) at 295 K.

Initial level	Final level	He		Ne	
		a	*b*	*a*	*b*
$6p[3/2]_2$	$6p[3/2]_1$	0.11 ± 0.04		0.004 ± 0.002	
	$6p[5/2]_3$	~ 0.06		~ 0.003	
	$6p[5/2]_2$			~ 0.003	
	$6p[1/2]_1$				
	$6s'[1/2]_1$			~ 0.003	
	$6s'[1/2]_0$			~ 0.003	
$6p[3/2]_1$	$6p[5/2]_3$	7.4 ± 0.6		0.013 ± 0.003	
	$6p[5/2]_2$				
	$6p[1/2]_1$			~ 0.002	
	$6s'[1/2]_1$			~ 0.002	
	$6s'[1/2]_0$			0.014 ± 0.004	
$6p[5/2]_3$	$6p[5/2]_2$	0.7 ± 0.3	0.75	0.10 ± 0.05	0.3
	$6p[1/2]_1$			0.12 ± 0.05	
	$6s'[1/2]_1$				
	$6s'[1/2]_0$				
$6p[5/2]_2$	$6p[1/2]_1$	0.5 ± 0.2	0.63	0.53 ± 0.10	0.69
	$6s'[1/2]_1$	0.2 ± 0.1		~ 0.001	
	$6s'[1/2]_0$				
$6p[1/2]_1$	$6s'[1/2]_1$	4.0 ± 2.0	< 0.2	0.02 ± 0.015	0.3
	$6s'[1/2]_0$	~ 0.001		~ 0.0001	
	$6s$			~ 0.0001	
$6s'[1/2]_1$	$6s'[1/2]_0$	~ 0.002		~ 0.0001	
	$6s$	~ 0.01		~ 0.0001	
$6s'[1/2]_0$	$6s$	~ 0.05		~ 0.005	

[a] This work.
[b] Xu and Setser (1991) (Ref. 12).

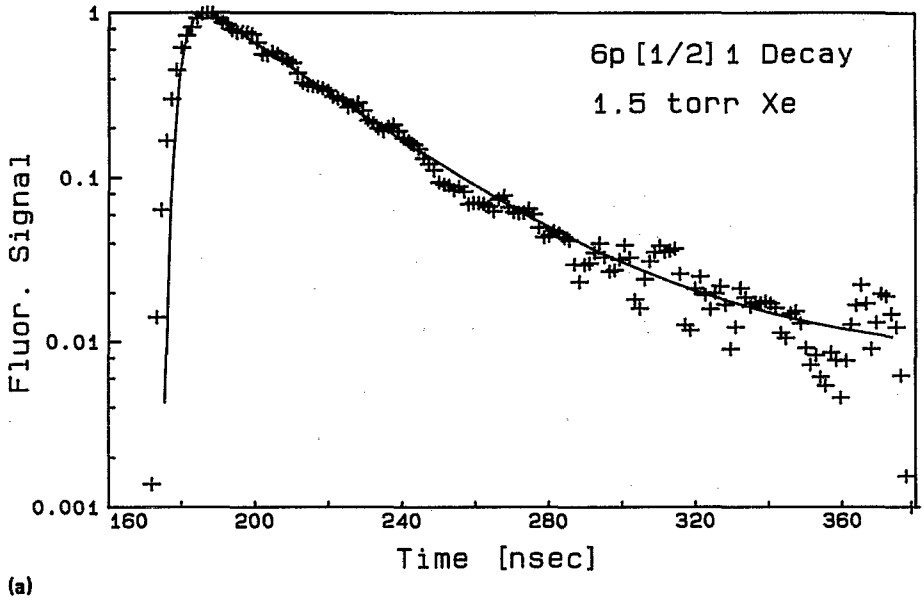

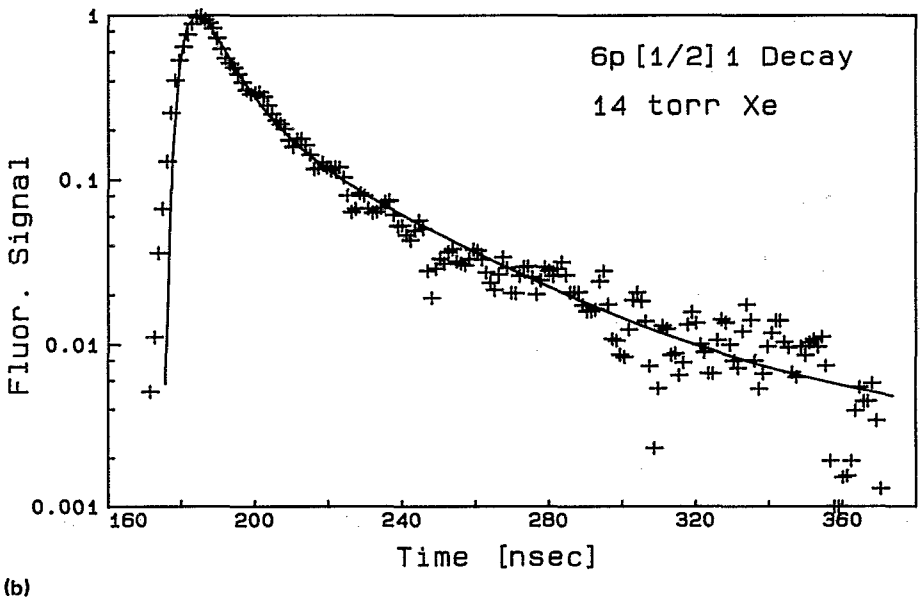

FIG. 6. Fluorescence decay of $6p[1/2]_1$ obtained for pumping $6p[1/2]_1$ at xenon pressures of (a) 1.5 and (b) 14 Torr.

$6s'[1/2]_1$ level, one does not see single-exponential decays when pumping $6p[1/2]_1$. This is due to the repopulation of $6p[1/2]_1$ after quenching to $6s'[1/2]_1$. This is demonstrated in Fig. 6 which shows fluorescence from $6p[1/2]_1$ with xenon as the quencher. Even at low pressures, a nonexponential decay is evident in Fig. 6(a) due to the strong coupling of the $[1/2]_1$ levels. The total rate constants for this level are obtained by fitting state-to-state rate constants to fluorescence decay data obtained at a variety of gas pressures. This would not be difficult if fluorescence from the $6s'$ levels was observed. Since it was not observed, we used the time dependence of the $6p[1/2]_1$ decay to infer the state-to-state quenching rate constants. For this reason, the uncertainties in the rate constants for the $6p[1/2]_1$ level are higher than other $6p$ levels. There are some obvious differences between our results for the $[1/2]_1$ levels and previous results. These will be discussed in the next section.

The rate constants for $6p[5/2]_3$ are also determined indirectly since this level was not directly pumped by the laser. By pumping the levels above and below $6p[5/2]_3$, i.e., $6p[3/2]_1$ and $6p[5/2]_2$, a self-consistent fit of the fluorescence data can be achieved. There are some problems with this procedure though. Generally, one needs to know either the total rate constant out of $6p[5/2]_3$ or the state-to-state rate constants to the nearest levels in order to get a precise, unique fit to the data. We take advantage of the fact (see Table V) that helium quenches $6p[3/2]_1$ much better than other levels and quenches almost exclusively to $6p[5/2]_3$. Thus we could pump $6p[3/2]_1$ and quickly transfer population to $6p[5/2]_3$ with helium collisions. By choosing appropriate pressures of helium and the quencher of interest, the decay of $6p[5/2]_3$ could be dominated by the gas of interest instead of the helium. Pumping $6p[3/2]_1$ then yields primarily information about the $6p[3/2]_1$ to $6p[5/2]_3$ rate

constant and the total rate constant out of $6p[5/2]_3$. Pumping $6p[5/2]_2$, one gets information about the $6p[5/2]_2$ to $6p[5/2]_3$ rate constant and some information about the $6p[5/2]_3$ total rate constant.

IV. DISCUSSION

We now discuss the state-to-state quenching rate constants for collisions with various rare gases, starting with xenon. In general, xenon shows a tendency to quench to a number of nearby levels and to the $6s'[1/2]_0$ level, which is $>1000\ \mathrm{cm}^{-1}$ lower in energy. Our rate constants are in reasonable agreement with the previous measurements of Ku and Setser[6] and Bowering *et al.*[4] with two noteworthy exceptions. The first is the disagreement in rate constants for $6p[3/2]_1$ and $6p[5/2]_3$ between the current work and the work of Ku and Setser.[6] They deduced a larger rate constant for $6p[3/2]_1$ to $6s'[1/2]_0$ and a smaller rate constant for quenching $6p[5/2]_3$ to $6p[1/2]_1$. These differences are due primarily to the larger total rate constant for quenching $6p[5/2]_3$ obtained in the present work. The $6p[5/2]_3$ total rate constant and state-to-state rates involving this level are obviously not independent since the state-to-state rates out of the level must sum to give the total rate. A larger total rate leads to larger state-to-state rates to this level from, e.g., $6p[3/2]_1$. Ku and Setser determined this total rate constant by directly pumping this level from the metastable $6s[3/2]_2$ level, but were restricted to pressures <5 Torr. Over this limited pressure ranch, only a $\sim 20\%$ change in $6p[5/2]_3$ decay rate was observed. Figure 7 shows some of the data we used to arrive at our larger rate constant for $6p[5/2]_3$. (The poor late-time fit of the $6p[3/2]_1$ data is again due to the low PMT voltage used.) The observed late-time decay of the $6p[5/3]_3$ fluorescence could not be fit by our model using

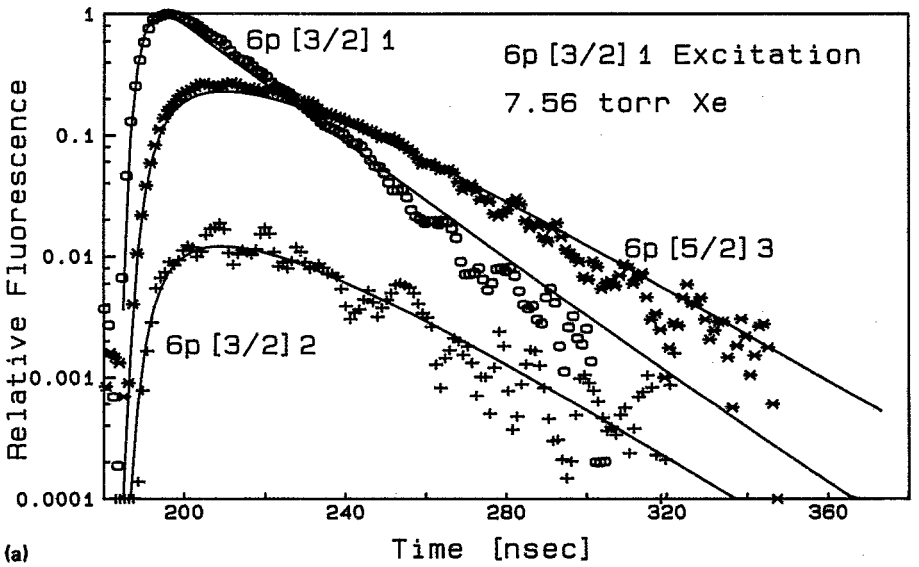

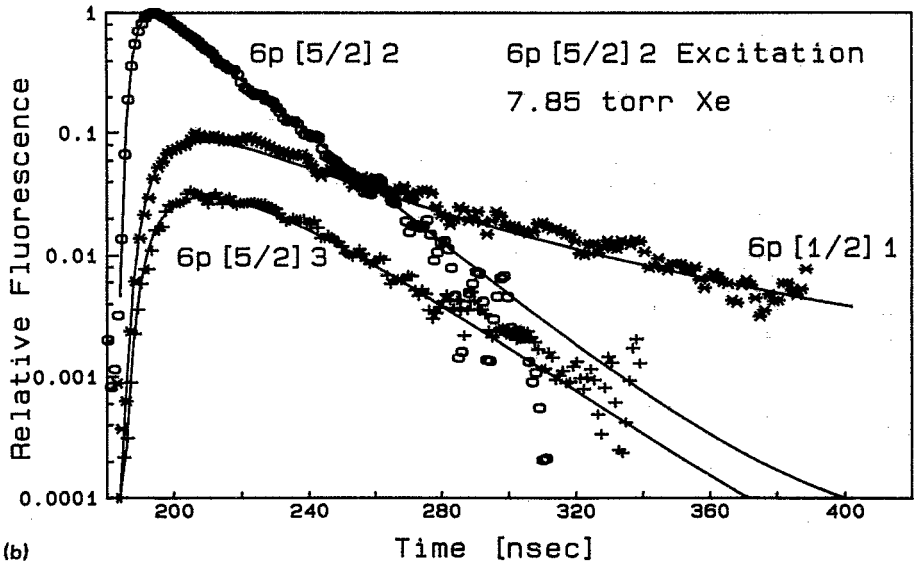

FIG. 7. Fluorescence at ~ 7.7 Torr of xenon for pumping (a) $6p[3/2]_1$ and (b) $6p[5/2]_2$.

the $6p[5/2]_3$ total rate constant of Ku and Setser. It should be noted that our data obtained by pumping $6p[5/2]_2$ could be fit using the lower $6p[5/2]_3$ rate constant, but the data obtained by pumping $6p[3/2]_1$ could not be well fit. This points out the importance of pumping as many levels as possible in order to obtain the most reliable results. If one pumps only a small number of levels and can adjust the total and state-to-state rate constants to fit the data, the system may be underdetermined.

The second noteworthy disagreement with previous results is the larger rate constant for quenching $6p[3/2]_2$ to $6s'[1/2]_1$ with xenon obtained by Bowering *et al.*[4] The present work and the work of Ku and Setser[6] did not find large rate constants for this process. Like us, Bowering *et al.* pumped the $6p[3/2]_2$ level and observed fluourescence from all 6*p* levels. When pumping this level, they observed no fluorescence from $6p[1/2]_1$. This would be consistent with our large rate constant for $6p[3/2]_2$ to $6s'[1/2]_0$ and small rate constant for $6p[3/2]_2$ to $6s'[1/2]_1$. One would expect a large $6p[3/2]_2$ to $6s'[1/2]_1$ rate constant to give rise to $6p[1/2]_1$ fluorescence due to the strong mixing of $6p[1/2]_1$ and $6s'[1/2]_1$. Populating $6s'[1/2]_0$ is expected to lead to weak $6p[1/2]_1$ fluorescence since the rate constants from $6s'[1/2]_0$ to $6p[1/2]_1$ and $6s'[1/2]_1$ are small ($< 10^{-12}$ cm^3 s^{-1}). The $6s'[1/2]_1$ level is the lowest excited level considered by Bowering *et al.*

Quenching of the $6s'[1/2]_{0,1}$ levels by xenon has been studied by Sadeghi and Sabbagh.[13] They obtain total quenching rates of $6.65 \pm 1.00 \times 10^{-11}$ and $8.45 \pm 0.85 \times 10^{-12}$ cm^3 s^{-1} for $6s'[1/2]_1$ and $6s'[1/2]_0$, respectively. Summing our state-to-state rates for these levels (upward as well as downward rates), we find total rate constants of $10.1 \pm 3.5 \times 10^{-11}$ and $1.1 \pm 0.5 \times 10^{-11}$ cm^3 s^{-1} for $6s'[1/2]_1$ and $6s'[1/2]_0$, respectively. The agreement with Sadeghi and Sabbagh is within experimental uncertainties.

The argon state-to-state rate constants also show a trend of quenching to a number of nearby levels. Our rate constants agree well with those of Xu and Setser[10] for $6p[5/2]_2$ and $6p[1/2]_1$, but differ significantly for $6p[3/2]_{1,2}$ and $6p[5/2]_3$. This is due largely to the smaller total rate constant we measured[11] for $6p[3/2]_1$ and the larger total rate constant we determined for $6p[5/2]_3$. For our measurements, we pumped $6p[3/2]_1$ and $6p[5/2]_2$ directly. Xu and Setser, however, pumped $6p[3/2]_2$ and $6p[5/2]_2$ to infer $6p[3/2]_1$ and $6p[5/2]_3$ decay rates. The discrepancy in rate constants is most noticeable for $6p[3/2]_2$ which we find quenches predominantly to $6s'[1/2]_1$, an interesting result given the > 1500 cm^{-1} change in energy. Another interesting observation is that argon only weakly couples $6p[1/2]_1$ and $6s'[1/2]_1$, which are separated by just 84 cm^{-1} and are strongly coupled by xenon (and helium).

The helium rate constants indicate a tendency to quench to the next lower level rather than many levels. The most prominent features of the helium rates are the large rate constants for coupling $6p[3/2]_1$ to $6p[5/2]_3$ and $6p[1/2]_1$ to $6s'[1/2]_1$. The only previous measurements of helium quench rates are the three of Xu and Setser.[12] We agree on two of the rate constants and disagree on the $6p[1/2]_1$ to $6s'[1/2]_1$ rate constant. Xu and Setser did not directly excite $6p[1/2]_1$. They deduced $6p[1/2]_1$ rates by pumping $6p[5/2]_2$ and observing $6p[1/2]_1$ fluorescence. Examples of fluorescence from $6p[1/2]_1$ obtained in our work, while pumping $6p[1/2]_1$ are shown in Fig. 8. A "fast" decay as well as a "slow" decay are observed. We attribute the fast decay to collisional quenching to the $6s'[1/2]_1$ level and the slow decay to quenching to levels below the $[1/2]_1$ levels. The $6p[1/2]_1$ and $6s'[1/2]_1$ can be equilibrated quite quickly at higher pressures, such as 162 Torr in Fig. 8, leaving only the slow decay of the two $[1/2]_1$ levels to lower levels.

The neon rate constants are all small and indicate that, unlike helium, neon quenches to a number of levels. The only previous measurements to compare with are three rate con-

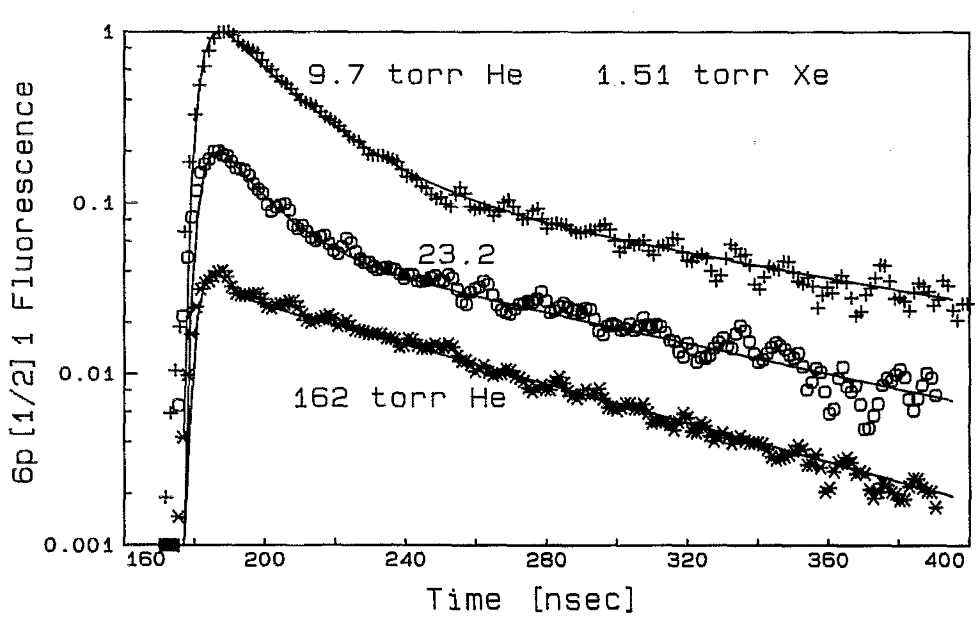

FIG. 8. Fluorescence decay of $6p[1/2]_1$ obtained when pumping $6p[1/2]_1$ at a xenon pressure of 1.51 Torr and helium pressures of 9.7, 23.2, and 162 Torr. The relative heights of the curves have been adjusted for clarity.

stants of Xu and Setser.[12] Again, we disagree on the $6p[1/2]_1$ to $6s'[1/2]_1$ rate constant, although we agree that the rate constant is rather small ($<4\times10^{-12}$ cm^3 s^{-1}). Our results indicate that neon has little effect on $6p[1/2]_1$ fluorescence decay unless the neon pressure is rather high (>500 Torr). Hence the very small rate constant for $6p[1/2]_1$.

The studies to date have provided a reasonable picture of the quenching of xenon 6p levels by rare gases. An exception is the quenching of the $6p[1/2]_0$ level. This level can be quenched to lower 6p levels as well as 5d levels which are difficult to observe. This problem requires more study. The quenching studies to date show total rate constants ranging over more than two orders of magnitude and state-to-state branchings varying greatly with the rare gas and 6p levels. Theoretical efforts to explain these interesting results by calculating the appropriate interatomic potentials and studying the coupling between various molecular states are under way.[21] Initial results have indicated a large rate constant for helium quenching $6p[3/2]_1$ to $6p[5/2]_3$, in agreement with experiment. Given the complexity of electronically excited xenon/rare-gas molecules, this is encouraging. One of the conclusions coming out of the calculations is that one needs potentials, the couplings between the potentials, and a calculation of the collision dynamics in order to determine quenching rates. One can not simply take the potentials and predict which rates will be large. We anticipate that these measurements and calculations will lead to a better understanding of collisional processes involving rare-gas excited states that play important roles in laser plasmas.

V. CONCLUSIONS

We have measured state-to-state and total quenching rate constants for the $6p[3/2]_{1,2}$, $6p[5/2]_{2,3}$, $6p[1/2]_1$, and $6s'[1/2]_1$ levels of xenon by helium, neon, argon, and xenon. This is the most comprehensive study to date of these levels. We have directly pumped four of the six levels studied and observed fluorescence from five of the six levels. Quenching by xenon gives large total rate constants $\sim10^{-10}$ cm^3 s^{-1} and usually couples a particular level to many nearby levels. Neon on the other hand has small total rate constants $<6\times10^{-12}$ cm^3 s^{-1} and also couples to a few nearby levels. Helium and argon show interesting variations in total rate constants for the 6p levels. For three of the 6p levels studied, argon has large rate constants, while helium has small rate constants. For the other two 6p levels studied, argon has small rate constants, while helium has large rate constants. The coupling of the closely spaced $6p[1/2]_1$ and $6s'[1/2]_1$ levels is large for helium and xenon, but small for neon and argon.

ACKNOWLEDGMENTS

The author would like to thank E. Ciszek for technical support. This work was performed at Sandia National Laboratories and was supported by the U.S. Department of Energy under Contract No. DE-AC04-76DP00789.

[1] H. Horiguchi, R. S. F. Chang, and D. W. Setser, J. Chem. Phys. **75**, 1207 (1981).
[2] A. W. McCowan, M. N. Ediger, and J. G. Eden, Phys. Rev. A **26**, 2281 (1982).
[3] G. Inoue, J. K. Ku, and D. W. Setser, J. Chem. Phys. **81**, 5760 (1984).
[4] N. Bowering, M. R. Bruce, and J. W. Keto, J. Chem. Phys. **84**, 709 (1986).
[5] N. Bowering, M. R. Bruce, and J. W. Keto, J. Chem. Phys. **84**, 715 (1986).
[6] J. K. Ku and D. W. Setser, J. Chem. Phys. **84**, 4304 (1986).
[7] P. Moutard, P. Laporte, N. Damany, J. L. Subtil, and H. Damany, Chem. Phys. Lett. **137**, 521 (1986).
[8] V. A. Karatazaev, Opt. Spectrosc. (USSR) **62**, 425 (1987).
[9] M. R. Bruce, W. B. Layne, C. A. Whitehead, and J. W. Keto, J. Chem. Phys. **92**, 2917 (1990).
[10] J. Xu and D. W. Setser, J. Chem. Phys. **92**, 4191 (1990).
[11] W. J. Alford, IEEE J. Quantum Electron. **26**, 1633 (1990).
[12] J. Xu and D. W. Setser, J. Chem. Phys. **94**, 4243 (1991).
[13] N. Sadeghi and J. Sabbagh, Phys. Rev. A **16**, 2336 (1977).
[14] M. Ohwa, T. J. Moratz, and M. J. Kushner, J. Appl. Phys. **66**, 5131 (1989).
[15] W. J. Alford, G. N. Hays, M. Ohwa, and M. J. Kushner, J. Appl. Phys. **69**, 1843 (1991).
[16] Chem. Phys. **145**, No. 2 (1990). Special Issue: *Dynamics of inelastic collisions of electronically excited atoms.*
[17] L. Krause, in *The Excited State in Chemical Physics*, edited by J. W. McGowan (Wiley, New York, 1975), p. 267.
[18] X. L. Han and J. F. Kelly, J. Chem. Phys. **94**, 5481 (1991).
[19] Y. J. Shiu, M. A. Biondi, and D. P. Sipler, Phys. Rev. A **15**, 494 (1977).
[20] M. Aymar and M. Coulombe, At. Data Nucl. Tables **21**, 537 (1978).
[21] A. P. Hickman, D. L. Huetis, and R. P. Saxon, J. Chem. Phys. (to be published).
[22] J. Sabbagh and N. Sadeghi, J. Quantum Spectrosc. Radiat. Transfer **17**, 297 (1977).
[23] M. M. Miller and R. A. Roig, Phys. Rev. A **8**, 480 (1973).
[24] R. G. Karimov and V. M. Klimkin, Sov. Phys. J. **14**, 308 (1971).
[25] V. P. Malakhov, Sov. Phys. J. **1**, 128 (1965).
[26] C. J. Chen and R. H. Garstang, J. Quantum Spectrosc. Radiat. Transfer **10**, 1347 (1970).